ISSN 1225-8024(Print)
ISSN 2288-8403(Online)

<연구논문>

한국표면공학회지
J. Korean Inst. Surf. Eng.
Vol. 50, No. 6, 2017.
https://doi.org/10.5695/JKISE.2017.50.6.427

Three-Dimensional (3D) Anodic Aluminum Surfaces by Modulating Electrochemical Method

Chanyoung Jeong[a,*] and Chang-Hwan Choi[b]

[a]Division of Advanced Materials Engineering, Dong-Eui University, 176 Eomgwangno, Busanjin-Gu, Busan 47340, Korea
[b] Department of Mechanical Engineering, Stevens Institute of Technology, Castle Point on Hudson, Hoboken, NJ 07030, USA

(Received December 6, 2017 ; revised December 17, 2017 ; accepted December 18, 2017)

Abstract

Anodic aluminum oxide (AAO) film has recently attracted much attention as a key material for the fabrication of various nanostructures. A control of anodizing voltage (U) was employed to render different anodic aluminum oxide (AAO) nanostructures with pore diameter (D_p) and interpore distance (D_{int}) in oxalic acid. In this work, we study the effect of stepwise modulation of anodizing voltages on the shape and dimension of porous structures along the vertical direction and demonstrate the fabrication of hierarchical layers of systematically controlled three-dimensional (3D) pore profile.

Keywords : Three-dimensional (3D) AAO nanostructures, Modulating voltage, Hierarchical alumina nanostructures

1. Introduction

Recently, an anodic alumina oxide (AAO) films with hexagonally packed pore arrays in nano-scale have attracted considerable attention in the nanotechnology field [1] although the AAO films formed by electrochemical anodization of aluminum in acid electrolytes has been extensively studied for 70 years [2]. Since the highly ordered AAO was developed by the two-step anodization process for fabricating self-ordered porous alumina templates, and these AAO films with desired pore size (Dp) and interpore distance (Dint) through anodization is the fundamental step that dominates the feasibility of the successive fabrication and the properties of resultant nanostructures [3,4]. The parameters of AAO films such as Dp and Dint will directly influence their performance in all these applications which has been applied to various functional nano-materials such as solar cells [5], chemical sensors [6], photonic nano-devices [7], metallic nano-wires [8,9], anti-corrosion [10] and etc. It is also possible to fabricate porous anodic alumina templates with a self-ordered hexagonal and periodic pore arrangement in a more cost-effective way than with other methods such as nanoidentation [11] and electron beam lithography [12]. However, it should be noted that most of the anodization methods were developed to form a two-dimensional (2D) porous array with the control of lateral dimensions only [13]. This work focused on the fabrication and structural control of three-dimensional (3D) AAO shapes. A control of anodization voltage (Ua) was employed to render different anodic aluminum oxide (AAO) nanostructures with pore size (Dp) and interpore distance (Dint) with in oxalic acid. Furthermore, a stepwise anodization with modulating voltages in oxalic acid was created to produce three-dimensional (3D) AAO nanostructures. The concept of modulating Ua both mild anodization (MA) at 40 V and hard anodization (HA) at 100 V has approached the stepwise of two different routes such as MA to HA, HA to MA mode.

*Corresponding Author: Chanyoung Jeong
Department of Advanced Materials Engineering, Dong-Eui University
Tel: +82-51-890-2286 ; Fax: +82-505-182-6896
E-mail: cjeong@deu.ac.kr

2. Experimental

A highly pure aluminum foils (99.9995%, Goodfellow Co., 1 cm × 3 cm × 0.05 cm) were first degreased in acetone and ethanol by ultra-sonication for 10 minutes and rinsed in deionized water. Subsequently, each specimen was electropolished to reduce surface irregularities in a mixture of perchloric acid and ethanol ($HClO_4/C_2H_5OH$ = 1:4 in volumetric ratio) under an applied potential of 20 V for 60 seconds. Aluminum was used as a working electrode and a platinum was used as a counter electrode in the anodization process. The two electrodes were separated at a distance of 5 cm. The typical anodization was conducted in a 0.3 M oxalic acid solution at 1°C with appropriate magnetic stirring (Fig. 1). The mild anodizing was applied at 40 V and the hard anodizing was applied at 100 V, respectively. The condition of AAO film removal is an aqueous mixture solution of 1.8 wt% chromic acid and 6 wt% phosphoric acid at 65°C for 10 hours. The cross-section morphology of the porous AAO films produced under different conditions was observed with a Scanning Electron Microscopy (Carl Zeiss). The specimens were cut into small pieces, mounted on a stage with carbon tape, and coated with a gold layer for 15 seconds by using sputter in order to SEM images observation clearly. For the examination of the cross-section of AAO, the specimen was bent into 90° to produce cracks parallel.

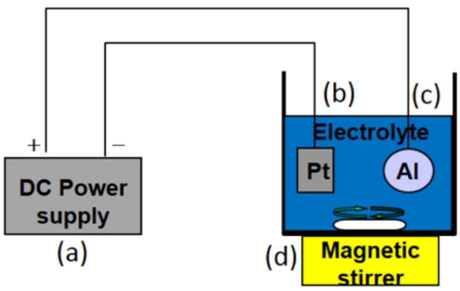

Fig. 1. Conventional anodizing set-up system. (a) DC Power supply, (b) Platinum as counter electrode, (c) Aluminum as working electrode, (d) Magnetic stirrer.

3. Results and discussion

3.1. Fabrication approach

Figure 2 shows the fabrication schematic of two-step anodization process. An aluminum foil is conducted to electro-polishing in order to both cleaning the surface and improving the pore arrangement. Without this step, non-uniform electric field due to irregular electrolyte/aluminum interface results in non-uniform pore penetration (Fig. 2a).

The first anodization step typically results in poor pore arrangement of aluminum oxide (Fig. 2b). Figure 2c shows the removal of the alumina layer using chemical etching for the second anodization

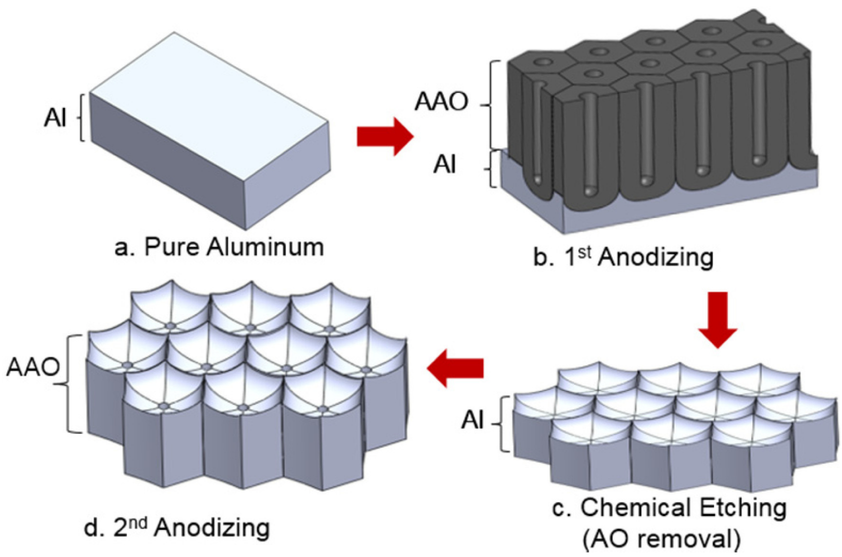

Fig. 2. Schematic of two-step anodization process. (a) Electro-polished aluminum substrate. Electro-polishing smoothens the surface and improves the pore arrangement. Without this step, non-uniform electric field due to irregular electrolyte/aluminum interface results in non-uniform pore penetration. (b) First anodization for initial pore arrangement. The first anodization step typically results in poor pore arrangement. (c) Chemical etching of the alumina layer for the second anodization step. (d) Well-ordered pore arrangement is obtained by the second anodization due to the pre-determined surface pattern remained after the chemical etching in the step (c).

step. The good uniform pattern was made to aluminum substrate through the removal step. Well-ordered pore arrangement is obtained by the second anodization due to the pre-determined surface pattern remained after the chemical etching in the step (c) (Fig. 2d). This pore structure is equivalent to conventional film and the thickness depends on the duration of the anodization process [14].

3.2. The effect of anodization voltage

The real samples are prepared by the electro-polishing and alternative anodization process such as stepwise mild and hard condition (Fig. 3) and the samples are inspected by SEM.

Figure 4 shows a set of SEM images of the fabricated MA to HA and HA to MA by one step anodizing process. For samples MA to HA and HA to MA, the anodization parameters such as the sort of electrolyte, temperature and concentration are experimental constant. In case of cross view images, AAO parameter was observed in terms of pore diameter (D_p) and inter-pore distance (D_{int}). The different pore diameter that results from the applied anodizing voltage employed was found between the MA and HA mode. Although it was hard to figure out the accurate D_p and D_{int}, the parameter shows a different scale both D_p and D_{int} as shown as Fig. 4. The D_p with MA to HA mode is much smaller than the D_p with HA to MA mode. The D_{int} with MA to HA mode also is much shorter than the D_{int} with HA to MA. Outer side of AAO is grown under MA condition, and inner side of AAO close to substrate is grown under HA condition.

Figure 5 represents also a set of SEM images of the fabrication with stepwise anodization voltage mode such as MA to HA and HA to MA with two step anodizing process, respectively. The process of two step anodizing would be obtained a better pore arrangement because of second time anodization. The second time anodization makes the pore arrangement

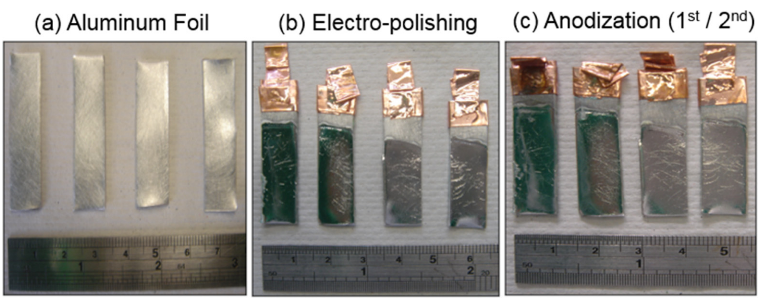

Fig. 3. Real samples. (a) Aluminum foils, (b) Electro-polished aluminum foils, (c) Anodized aluminum foils.

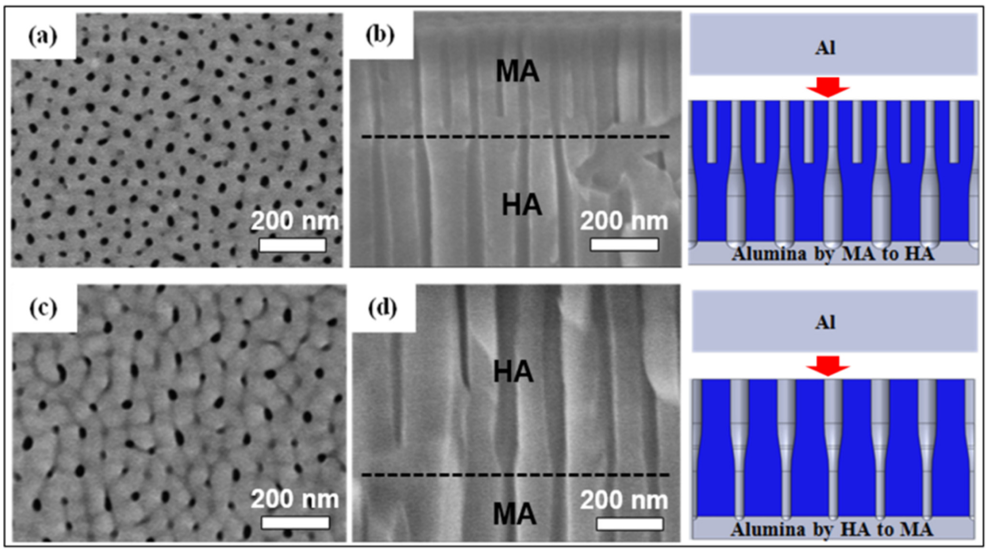

Fig. 4. SEM images of top and cross-sectional morphologies of AAO film with 3D structures formed with different anodization voltage (formed by one-step anodizing process) and schematic diagram of multi-pore structure (formed by one-step anodizing process). (a) Mild anodizing to hard anodizing (MA to HA), (b) Hard anodizing to mild anodizing (HA to MA).

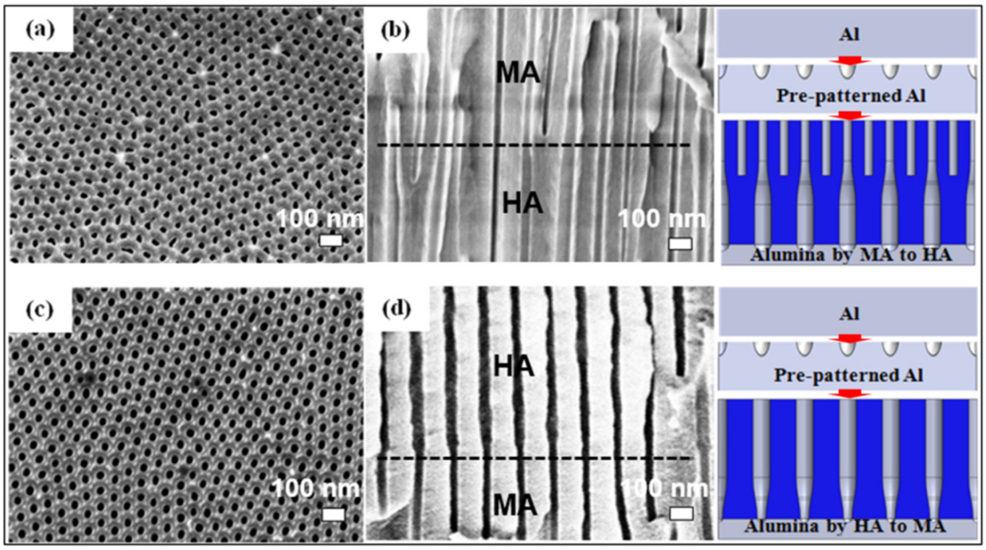

Fig. 5. SEM images of top and cross-sectional morphologies of AAO film (formed by two-step anodization) and schematic diagram of multi-pore structure in single alumina capsule. (a) Mild anodizing to hard anodizing, (b) Hard anodizing to mild anodizing.

to much better uniformity than first time one since the uniform pattern on aluminum directly was established for the first time anodization step. The sample that was conducted by second time anodization shows a precise the size of D_p and D_{int} than the mode of first time anodization such as Fig. 4. In case of top view images, the D_p of MA to HA mode is much smaller than that of the mode of HA to MA as shown as in Fig. 5. Therefore, the major different of AAO structural parameters between one-step and two-step anodizing processes is a pore uniformity. And the surface morphology only reflects the approach of first time mode (MA or HA) condition regardless of the following anodizing mode (HA or MA). Some structural variation of AAO was induced by modulating voltage, and that can be observed in cross-sectional images.

4. Conclusion

Here, we show the control of AAO structures not only D_p and D_{int} but also hierarchical three-dimensional AAO nanostructures by stepwise anodization with modifying *U*a. This work allows one to accomplish a selective control of the AAO structures during their growth, aiming for the production of multi-component nanostructures. In conclusion, the results demonstrate that the 3D vertical morphology of the porous aluminum oxide layer can be systematically modulated by controlling the anodizing modes (e.g., voltages). Such hierarchical nanoporous structures with tunable vertical profiles would benefit many applications with tailored materials/surface properties and system/device functionality.

Acknowledgement

This work was supported by the National Research Foundation of Korea (201704140001) and the Dong-Eui University Grant (201702670001). The authors would like to thank Prof. Keith Sheppard at Stevens Institute of Technology for motivating the idea investigated in this work.

References

[1] H. Masuda and K. Fukuda, Ordered Metal Nanohole Arrays Made by a Two-Step Replication of Honeycomb Structures of Anodic Alumina, Science, 268 (1995) 1466-1468.
[2] F. Keller, M.S. Hunter, and D.L. Robinson, Structural Features of Oxide Coatings on Aluminum Journal of The Electrochemical Society, 1953. 100 (1953) 411-419.
[3] F. Li, L. Zhang, and R.M. Metzger, On the Growth of Highly Ordered Pores in Anodized Aluminum Oxide, Chemistry of Materials, 10 (1998) 2470-2480.
[4] A. P. Li, F. Muller, A. Birner, K. Nielsch and U. Gosele, Hexagonal pore arrays with a 50–420 nm interpore distance formed by self-organization in anodic alumina, Journal of Applied Physics, 84 (1998) 6023-6026.

[5] N. Haberkorn, J.S. Gutmann, and P. Theato, Template-assisted fabrication of free-standing nanorod arrays of a hole-conducting cross-linked triphenylamine derivative, ACS Nano, 3 (2009) 1415-1422.
[6] S.A.A. John H. Holtz, Polymerized colloidal crystal hydrogel films as intelligent chemical sensing materials, Nature, 389 (1997) 829-832.
[7] M. Deubel, G. Von Ferymann, M. Wegener, S. Pereira, K. Busch and C. M. Soukoulis, Direct laser writing of three-dimensional photonic-crystal templates for telecommunications, Nat Mater, 3 (2004) 444-447.
[8] G. Sauer, G. Brehm, S.Schneider, K. Nielsch, R. B. Wehrspohn, J. Choi, H. Hofmeister and U. Gosele, Highly ordered monocrystalline silver nanowire arrays, Journal of Applied Physics, 91 (2002) 3243-3247.
[9] J. Choi, G. Sauer, K. Nielsch, R. B. Wehrspohn and U. Gosele, Hexagonally Arranged Monodisperse Silver Nanowires with Adjustable Diameter and High Aspect Ratio, Chemistry of Materials, 15 (2003) 776-779.
[10] F. Zhang, L. Zhao, H. Chen, S. Xu, D. G. Evans and X. Duan, Corrosion Resistance of Superhydrophobic Layered Double Hydroxide Films on Aluminum, Angewandte Chemie International Edition, 47 (2008) 2466-2469.
[11] S. Kwon, X. Yan, A. M. Contreras, J. A. Liddle, G. A. Somorjai and J. Bokor, Fabrication of Metallic Nanodots in Large-Area Arrays by Mold-to-Mold Cross Imprinting (MTMCI), Nano Letters, 5 (2005) 2557-2562.
[12] D. Routkevitch, A. A. Tager, J. Haruyama, D. Almawlawi, M. Moskovits and J. M. Xu, Nonlithographic nano-wire arrays: fabrication, physics, and device applications, IEEE Transactions on Electron Devices, 43 (1996) 1646-1658.
[13] A. Santos, J. Ferre-Borrull, J. Pallares, and L. F. Marsal, Hierarchical nanoporous anodic alumina templates by asymmetric two-step anodization, Phys. Status Solidi A, 208 (2011) 668-674.
[14] T. Nagaura, F. Takeuchi, and S. Inoue, Fabrication and structural control of anodic alumina films with inverted cone porous structure using multi-step anodizing Electrochimica Acta, 53 (2008) 2109-2114.